Are Simple Calculation Models always on the Safe Side?

Univ. Prof. Dr.-Ing. Jean-Marc Franssen *

* University of Liege, Structural Engineering dpt, Belgium, jm.franssen@ulg.ac.be

Abstract:

This paper examines the question whether simple calculation models are always on the safe side compared to advanced calculation models. This question is examined for the shadow effect, for the contact between steel and concrete in composite steel-concrete floors, for the buckling curves of steel sections and, finally, for the factors κ1 and κ2 applied to the bending resistance of steel beams.

Keywords: simple calculation model, advanced calculation model, fire

1 Introduction:

Eurocode 3 for the design of steel structures subjected to fire [1] mentions three different levels of calculation methods, namely tabulated data, simple calculation models and advanced calculation models.

Tabulated data, based on tests or advanced calculation models, are not really present in Eurocode 3. It is expected that tabulated data may emerge in the form of design aids that will be prepared in the future by interested external organizations.

Advanced calculation models are design models in which engineering principles are applied in a realistic manner to specific applications. They should be based on fundamental physical behaviour and provide a realistic analysis of structures exposed to fire.

Simple calculation models are design methods for individual members, which are based on conservative assumptions.

This paper examines this question whether simple calculation methods are systematically on the safe side compared to advanced calculation models, as implied by the definition of simple calculation model given in the Eurocode. It will be shown that, in fact, there are several aspects for which this is not the case.

2 Shadow factor

The flux at the surface of an unprotected steel element is given by Eq. (1).

$$\dot{h_{net}} = \alpha_c(\theta_g - \theta_m) + \emptyset\, \varepsilon_m\, \varepsilon_f(\theta_r^4 - \theta_m^4) \tag{1}$$

where Φ is the configuration factor, normally taken as 1,0 although it is mentioned that a lower value could be chosen to take account of the shadow effect.

In convex sections, Φ is indeed taken as 1,0 and Eq. (1) is applied as such in Eq. (2) for calculating the temperature in unprotected sections with the simple calculation model.

$$\Delta\theta_m = k_{sh}\, \frac{A_m/V}{c_m \rho_m}\, \dot{h_{net}}\, \Delta t \tag{2}$$

Eq. (1) is also used in advanced calculation models. As a consequence, the uniform temperature calculated with a simple calculation model is very close to the average value of the temperatures calculated with the advanced calculation model.

For concave sections, it can be shown that the amount of radiative energy that crosses the so called "box section", i.e. the smallest convex section that can encompass the real section, cannot have increased when it meets the surface of the steel element. For convection, on the other hand, and except in very closed cavities (e.g. in *Hollerith* composite profiles), mass transfer provided by air circulating in the concave re-entrant parts of the section can bring in energy and, finally, the convective heat transfer in these cavities is of the same order of magnitude as the one that occurs on the convex parts of the section. A modification should thus happen essentially on the radiative part of the net het flux.

Yet, it has been decided in Eurocode 3 not to use the possibility to choose values of Φ lower than 1,0 in Eq. (1); A correction factor k_{sh} calculated by Eq. (3) in most cases is applied on both terms of the net heat flux given by Eq. (1), the convective term as well as the radiative term.

$$k_{sh} = \frac{A_{m,b}}{A_m} \tag{3}$$

This approximation has been introduced because it allows keeping one single geometrical parameter to represent each section (namely, the ratio $A_{m,b}/V$) instead of two (namely A_m/V and Φ) if the correction is applied only on the radiative part of the flux. The approximation is justified because the convective heat flux is smaller than the radiative flux in

Eq. (1). Typical values for sections heated by the ISO curve show that the radiative flux is quickly equal to 5 or more times the convective flux. Yet, this approximation is not on the safe side compared to Eq. (1).

Another factor 0.9 is even applied in the calculation of k_{sh} for I-sections under nominal fire actions. The origin of this factor and why it is limited to I-sections under nominal fire actions are unknown to the author of this paper.

If, applying the advanced calculation model in a numerical analysis, the fire curve is applied on the whole perimeter of the section in a way that the heat flux is calculated according to Eq. (1) on the whole perimeter, the protection to radiation provided by the concave nature of the section is not considered and the advanced model will yield temperatures that are higher than the simple calculation model.

In order to illustrate the discussion, some calculations have been performed under ISO fire with a section that has the properties of HE200B, namely $A_m/V = 147,2$ and $A_{m,b}/V = 102,4$. The results are presented in Figure 1.

If the simple model is applied with the flux calculated with the assumption that the concave shape has an influence only on the radiative flux, then Eq. (1) is used with $\Phi = A_{m,b}/A_m = 102,4 / 147,2 = 0,696$ and k_{sh} is taken as 1,0 in Eq.(2). The results are presented as a thick line under caption "SM – phi" in Figure 1. The temperature after 30 minutes is 780°C.

If now the approximation is made that the influence of the concave shape is applied on both terms of Eq. (1), convective as well as radiative, then Φ is taken as 1,0 in Eq. (1) but $k_{sh} = 0,696$ is used in Eq(2). The results are shown as a dotted line under caption "SM – Am,b" on Figure 1. The temperature after 30 minutes is 771°C (-1,1%).

If, in addition, the factor 0.9 is introduced, k_{sh} in Eq. (2) will be taken as 0,626 and the thin line under caption "SM – EC3" in Figure 1. The temperature after 30 minutes is 756°C (3,1%).

If the advanced calculation model is applied with Eq (1) applied on the whole perimeter and $\Phi = 1,0$, the highest dotted line under caption "AM" of Figure 1 is obtained. The temperature after 30 minutes is 813°C (+4,2%).

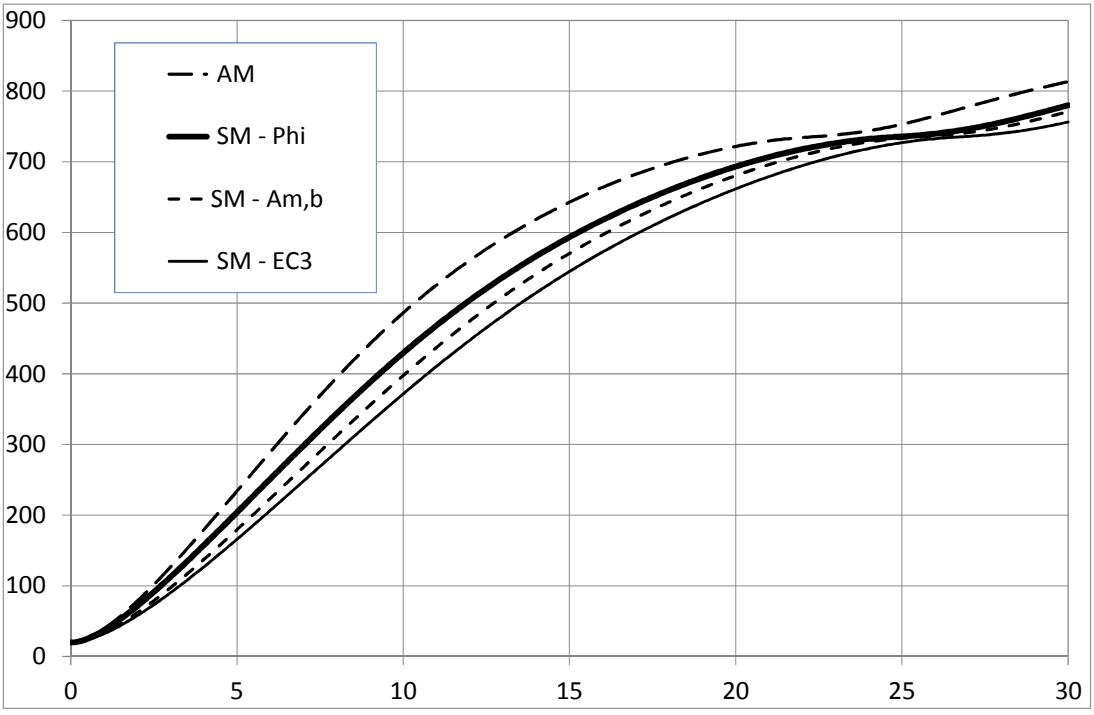

Figure 1: Temperature evolution with different models

Other values will be obtained with different situations. The differences between the results obtained with different hypotheses are higher for massive sections, short fire resistance times and highly concave shapes. They are reduced for thin sections, long fire resistance times and less concave shapes.

Different techniques exist that allow considering the concave nature of the section in advanced calculation models. The most simple ones rely on a modification of the boundary properties of the material that appear in Eq. (1): coefficient of convection and/or emissivity. The modification can be made with average values for the whole section but it is also possible to differentiate for different boundaries of the section, for example convex part of the section on one hand (with no modification on this part) and concave part of the section on the other hand. Also the concave part can be differentiated, e.g. between the web and the interior sides of the flanges for an H section.

3 Steel-concrete composite floors

When two different materials are adjacent in a numerical model, the usual finite element formulation considers a perfect contact between the two materials; there is no resistance to heat transfer by conduction at the interface.

In composite steel-concrete floor systems based on trapezoidal or re-entrant cold formed steel sheets supporting fresh concrete in the construction stage, the steel sheet and the concrete are really in direct contact (this is in fact a condition for the two materials working together and developing a composite action) and the model represents correctly the behaviour for normal temperatures.

In the fire situation yet, the steel sheets tend to de-bond and detach from the concrete slab. This has been observed in many experimental tests. This will introduce a resistance to conduction between the two materials (the presence of the "insulating" air gap is often mentioned in the literature). This resistance will lead to slightly higher temperatures in the steel sheet, but this is not very detrimental for the fire resistance of the system because the temperature of the steel sheet is very high anyway and this element hardly contributes to the load bearing capacity. The additional resistance will on the other hand be beneficial for the temperatures in the concrete slab. The load bearing capacity will be improved because of the delayed heating of the re-bars that are usually present in the slab. The insulting capacity of the system will also be improved because of the delayed temperature increase on the upper unexposed surface.

As an example, the composite floor system represented on Figure 2 has been analysed numerically for different thickness of the concrete slab put over the upper flange of the steel profile (the concrete thickness of Figure 2 is 120 mm). The steel profile is COFRAPLUS 200 from ArcelorMittal with a thickness of the steel sheet equal to 1,0 mm.

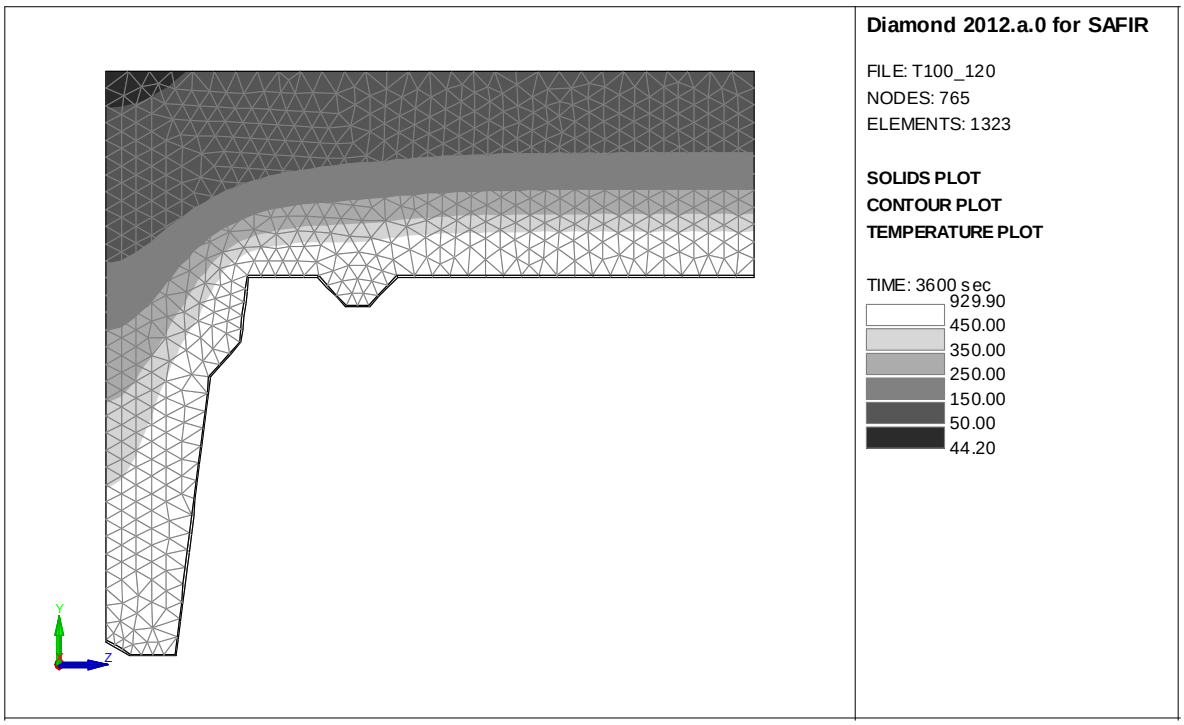

Figure 2: Temperature distribution in a composite floor system

Figure 3 presents the fire resistance time calculated by the advanced model SAFIR [2] on the base of the insulating criteria I as a function of the thickness of concrete over the slab (curve with caption "AM "). On the same graph are presented the points given in Table D.6 of Eurocode 4 [3] (caption "EC4"). It has to be noted that, strictly speaking, the dimensions of the steel profile do not fit within the limits of applicably for simple methods given in Table D.7 of the Eurocode. Nevertheless, according to clause D.4 (2), when the width of the upper flange of the section is more than twice the width of the lower flange, which is the case here, the thickness of concrete cover on the upper flange can be considered as the effective width and, as a consequence, used with Table D.6. The comparison is thus valid to judge from the influence of the thermal resistance between the steel section and the concrete.

For this geometry of the steel profile, there is a rather good agreement between the advanced calculation model and the simple calculation model except, perhaps, for low thicknesses. The results of the simple model are the same or are on the safe side compared to those of the advanced model. It has yet to be mentioned that this result has been obtained by

considering the effect of the concave shape of the section in the numerical analyses. For the central part of the upper web for example (between the two stiffeners present on the edge of this upper flange), the heat flux as given by Eq. (1) has been calculated with a factor $\Phi = 0{,}786$ (the emissivity of the material has been reduced from 0.70 to 0,55. No reduction of the convective flux has been considered.

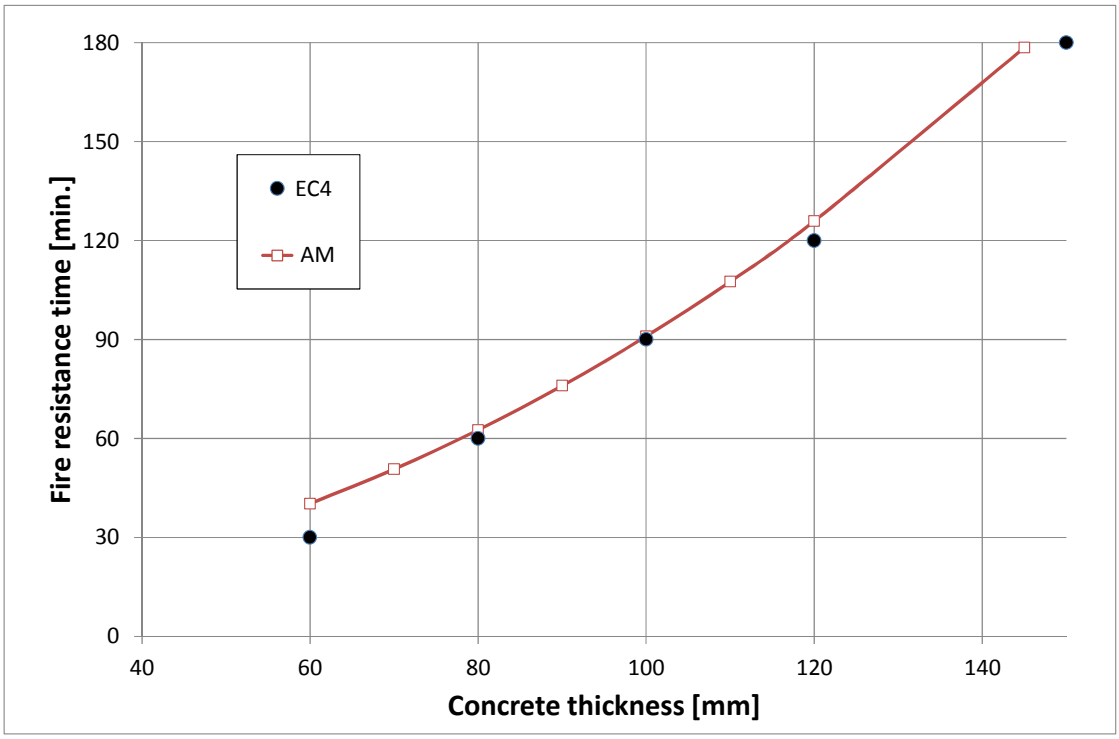

Figure 3: Fire resistance time as function of the concrete thickness

In his Ph. D. thesis [4], Renaud has analysed the thermal resistance that appears in hollow filled sections and was able to quantify it. It is thus possible to introduce in advanced models a thin layer of fictitious material that hast provides this thermal resistance. It has to be recognised that hollow sections are usually made of thicker steel plates and exhibit less deformations, except at the very late stage before collapse, than those exhibited by the thin steel sheets of composite floors. For the latter case, the variability of the phenomenon is much higher which makes it difficult to quantify it.

From these considerations, the strategy of the author is to model the thermal resistance between steel and concrete for hollow sections filled with concrete but not for composite floors. In composite floors, the concave nature of the section is considered by reducing the radiative heat flux in the concave parts of the section.

4 Buckling curves

A buckling curve is presented in Eurocode 3 to be used in the simple model for the fire resistance of steel columns.

The shape of this curve, the equation that would represent it as well as the parameters that would be considered in the equation have been obtained from an extensive campaign of some 200 000 numerical simulations made with the advanced model [5]. When the equation obtained from the simulations were compared with a data base of experimental test results, it was observed that the numerical results and the experimental results showed the same response as a function of the relevant parameters but the numerical results were, generally, slightly lower than the experimental results [6]. This was attributed to the fact that both the geometrical imperfections as well as the residual stresses had been considered with their characteristic values in the simulations whereas the probability of the simultaneous occurrence of the characteristic for both factors is very low. As a consequence, the buckling curve was calibrated to better represent the experimental results; the imperfection factor used in the buckling curve was set to 0,65, see Eq. 4.6 of Eurocode 3.

Now, if a steel column is modelled in an advanced calculation model, it is not known which level of imperfections have tp be modelled to obtain the same results as the simple calculation model (these supposed to correspond to the experimental results). It would be interesting if only a geometric imperfection of given amplitude could yield this result because the introduction of a residual stresses pattern in a model is more complex than the introduction of an initial

imperfection. Whether this is possible and, if so, what is the amplitude of the required imperfection is not known to the author.

The buckling curve for steel members in compression has been exclusively determined from numerical analyses and experimental results made on hot rolled H or I sections. Yet, they are applied as such for all sections types, welded sections, hollow steel sections, angles, U or C sections. The applicability of the buckling curve for all these sections types has not been verified. It would then not come as a surprise that the results provided by advanced model calculations would be different from those given by the simple model. Whether the results would be close or not and which one would be more conservative than the other has not been investigated. In the team of the author and, approximately at the same time, in the team of Professor Schaumann (private communication), some results obtained numerically on columns with non-conventional sections types, have been found to be significantly different from those provided by the buckling curve of the Eurocode but this question has not been investigated thoroughly.

5 κ2 factor

According to clauses (3) and (8) of section 4.2.3.3 of Eurocode 3, the plastic bending resistance of class 1 and class 2 members can be divided by a factor $\kappa 2 = 0,85$ at the supports of statically indeterminate beams. The plastic bending resistance is thus 1,18 times higher on the supports than the value calculated on the base of a temperature distribution that is not disturbed by the supports. This effect is not represented as such in an analysis performed with an advanced model, namely with a numerical model based on beam finite elements.

It can easily be calculated in the load domain that, at a given requested fire resistance time, the load bearing capacity of a central span in a continuous beam supporting a uniformly distributed load is equal to

$$P = 16\ M_{pl}/L^2 \tag{4}$$

if there is no favourable effect on the supports whereas it is equal to

$$P = 8\ (1+1,18)\ M_{pl} / L^2 = 17,4\ M_{pl}/L^2 \tag{5}$$

if the factor κ2 is taken into account on the supports, with M_{pl} the plastic resistance in the span.

The first result is likely to be provided by the advanced model and the second one by the simple calculation model. There is thus an additional safety margin provided by the advanced model compared to the simple model.

It can easily be calculated that the effect of increasing the bending resistance on the supports is equivalent to a reduction of the span to $(16/17,4)^{0.5} = 96\%$ of the theoretical distance between the supports. This means that the advanced model would yield the same answer as the simple model if a length of 2% of the span is left unheated from each support (slightly different figures would be calculated for the end spans of a continuous beam).

The discussion above is based on the hypothesis that the advanced model analysis will detect plasticity exactly on the supports which means, for the beam finite element, that yielding is evaluated at the ends of the element. This will be the case if, for instance, the longitudinal integration is performed with a Lobatto integration scheme. If, on the other hand, integration is performed by a Gauss integration scheme as is the case for SAFIR, the first point where yielding is evaluated is close to the supports, but not exactly on the supports. For example, with two point of integrations on the length of the element, the first point is approximately at a distance of $0,2\ \ell$ from the end of the element, with ℓ being the length of the finite element. If 10 beam finite elements are used on the length of the beam, then $\ell = L/10$ and yielding will be evaluated at a distance of 0,02 L from the support, which is exactly the value giving the increase of capacity provided by the favourable effect from non-uniform temperature on the supports.

6 κ1 factor

According to clauses (3) and (7) of section 4.2.3.3 of Eurocode 3, the plastic bending resistance of class 1 and class 2 members can be divided by a factor $\kappa 1 = 0,70$ for unprotected beams exposed on 3 sides with a concrete slab on side four, which means on the upper side of the upper flange (the factor is 0,85 for protected beams). This factor is applied to the reference bending resistance that is calculated on the base of the temperature distribution that does not take the slab into account.

In fact, the slab is taken into account in the temperature distribution for the reference bending resistance by considering the fact that the upper side of the steel section is not affected by the fire; an adiabatic boundary condition is assumed to

exist on this surface and, as a consequence, the section factor A_m/V of the section is reduced compared to that of a section heated on 4 sides.

The factor κ1 stems from the fact that the slab has another effect on the temperature distribution. Not only does it protect the upper flange from the application of the fire, but it also absorbs heat from the flange for its own heating. Heat is transferred from the flange to the concrete slab that acts as a heat sink.

This thermal effect can easily be reproduced in thermal analyses performed with an advanced thermal model; instead of just representing the steel section with an adiabatic boundary, the concrete slab is introduced in the model. When this is done, it is indeed observed that the temperature in the upper flange is lower compared to the situation when the slab is not modelled. For example, Figure 4 presents the temperature distribution calculated after 30 minutes of ISO fire in an unprotected IPE300 section, on the left with the upper slab in the model and on the left with an adiabatic boundary condition. The temperature in the upper flange is reduced from 780 to 690° when the slab is taken into account.

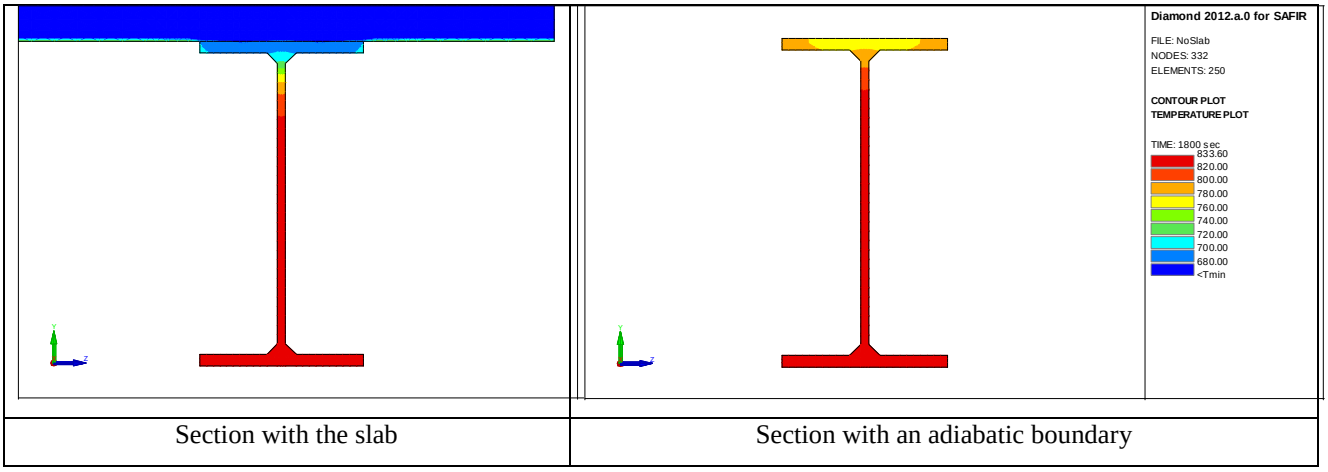

Section with the slab	Section with an adiabatic boundary

Figure 4: Temperature distribution with two different models

Yet, dividing the bending strength by 0,70 amounts to multiply the strength by 1,43 and such an increase cannot be observed in the mechanical analyses performed with advanced models. The reason is that the increase of compression capacity provided to the upper flange does not add much to the bending capacity of the section if the tensile capacity of the lower flange is kept the same (the temperature in the lower flange is, in Figure 4, around to 825°C in both cases). It is equivalent to increase the compression capacity of a reinforced concrete beam that has been designed to fail at the same time by tension in the steel bars and by compression in the concrete; failure will occur for a very similar bending moment, by tension in the bars. In the steel beams, there is a slight effect because the cooling extends somehow in the web, but by no way can this lead to an increase of bending capacity of more than 40%. For example, if the sections of Figure 4 are used in a 5 meters simply supported beam, the load bearing capacity after 30 minutes of fire calculated by a non-linear finite element analysis is increased from 7,97 kN/m when the slab is replaced by an adiabatic boundary condition to 856 kN/m when the slab is considered in the thermal model (the slab is not acting in a composite action with the steel beam). The increase is for this example of 7,4%, equivalent to a value of the coefficient κ1 equal to 0,93. Other values would be obtained with other geometries.

To the knowledge of the author, there is no way that the advanced model can yield the strength increase allowed for by the simple model.

The aim of the discussion was to highlight the possible difference between advanced and simple calculation models. Another question is which model better describes the behaviour of steel sections in experimental tests or in real structures under fire. It is possible that a concrete slab supported on a steel section will develop some level of composite action that, perhaps, can be activated in accidental actions and can explain lower values of κ1 factors used in the simple model.

7 References

[1] EN 1993-1-2, *Eurocode 3: Design of steel structures – Part 1-2: General rules – Structural fire design*, CEN, Brussels, 2005.

[2] Franssen, J.-M. *SAFIR: A thermal/structural program for modeling structures under fire*. Engineering Journal,- American Institute of Steel Construction Inc, 42(3), 143-158, 2005.

[3] EN 1994-1-2, *Eurocode 4 – Design of composite steel-concrete structures – Part 1-2: General rules – Structural dire design*, CEN, Brussels, 2005.

[4] Renaud, C., *Modélisation numériques, expérimentation et dimensionnement pratique des poteaux mixtes avec profil creux exposés à l'incendie*, Ph. D. thesis, INSA, Rennes, 2003.

[5] Talamona, D, Franssen, J.-M, Schleich, J.-B, & Kruppa, J. *Stability of Steel Columns in Case of Fire : Numerical Modelling*. Journal of Structural Engineering, 123(6), 713-720, 1997.

[6] Franssen, J.-M, Talamona, D, Kruppa, J, & Cajot, L.-G. *Stability of Steel Columns in Case of Fire : Experimental evaluation*. Journal of Structural Engineering, 124(2), 158-163, 1998.